Effect of carrier gas on the structure and electrical properties of low dielectric constant SiCOH film using trimethylsilane prepared by plasma enhanced chemical vapor deposition

Y.L. Cheng[a],*, Y.L. Wang[b,c], J.K. Lan[b], H.C. Chen[b], J.H. Lin[b],
Y.L. Wu[c], P.T. Liu[d,e], Y.C. Wu[a], M.S. Feng[a]

[a]Department of Material Science and Engineering, National Chiao-Tung University, Hsin-Chu, Taiwan, ROC
[b]Taiwan Semiconductor Manufacturing Co., Ltd, Hsinchu, Taiwan, ROC
[c]Department of Electrical Engineering, National Chi-Nan University, Nan-Tou, Taiwan, ROC
[d]Department of Photonics of Display Institute, National Chiao-Tung University, Hsin-Chu, Taiwan, ROC
[e]National Nano Device Laboratory, 1001-1, Ta-Hsueh Rd, Hsin-Chu, Taiwan, ROC

Abstract

For a low dielectric constant inter-metal dielectric application, the low-k SiCOH film with a dielectric constant of 2.8–3.2 has been deposited by plasma-enhanced chemical vapor deposition (PE-CVD) with trimethylsilane (3MS), oxygen, and the carrier gas. In this work, we present the effects of the carrier gas on the characterizations of the low-k films, including reaction mechanism, the deposition rate, and the mechanical and electrical properties. According to the experimental results, the low-k film in Ar carrier gas exhibits the improvement in deposition rate, nonuniformity, leakage current, and hardness. In addition, the dielectric constant of the deposited low-k film is slightly sacrificed due to the decrease of micropores in the deposited films.
© 2004 Elsevier B.V. All rights reserved.

Keywords: Low-k; Carrier gas; Plasma-enhanced chemical vapor deposition

1. Introduction

The continuous shrinkage of the device dimensions of the ultralarge-scale integrated (ULSI) chips imposes strong demands on the backend of the line (BEOL) interconnect structure. Low-dielectric-constant (low-k) SiCOH materials are required in the interconnect structure to reduce parasitic capacitance of multilevel interconnects, cross-talk noise between metal wires, and power dissipation from the RC coupling [1–3]. For these reasons, strong efforts have been conducted to find a suitable insulator material with a dielectric constant about 2.8–3.2.

There are intense industry-wide efforts to develop low-k materials as interlayer dielectrics. It is well known that the incorporation of carbon into SiO_2 would decrease its dielectric constant. Carbon-doped low-k films are usually deposited by plasma-enhanced chemical vapor deposition (PE-CVD) from a mixture of trimethylsilane [3MS, $(CH_3)_3SiH$] or tetramethylsilane [4MS, $(CH_3)_4Si$] with oxygen [4–8]. However, there is a trade-off between the dielectric constant and mechanical strength of these low-k films. A low-k film with a lower dielectric constant usually accompanied with a weaker mechanical strength and vice versa. As a result, optimization of the process conditions is inevitable for meeting the low-k film requirements, including a lower dielectric constant and an improved mechanical strength.

In this paper, different carrier gases were added during the deposition process of the low-k film with 3MS and O_2 as the reaction gases in a PE-CVD system. The influence of carrier gas on the physical properties (thickness and refractive index), structure properties, electrical properties

---

Gas Phase Reaction:

Reaction gas :   **Intermediates** :

$(CH_3)_3SiH + O_2 \longrightarrow (CH_3)_3Si^+, CH_3Si^{3+}, O^{*\cdots\cdots}$

Diffusion of by-product

Gas Phase Diffusion:
O_2 , Carrier gas (Ar, He)
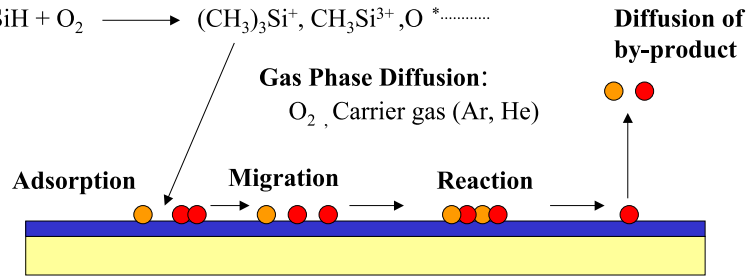
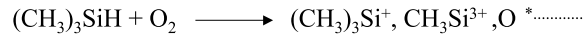**Adsorption**   **Migration**   **Reaction**

Fig. 1. A series of reaction process steps of the low-*k* film formation using 3MS and O_2.

(dielectric constant and breakdown voltage), and mechanical strength of the low-*k* films are investigated.

2. Experimental procedures

A low-*k* film was deposited from trimethylsilane and oxygen using radio frequency 13.56 MHz plasma on an Applied Materials Producer system with a 200 mm chamber. Two different carrier gases (He, Ar) were used with the flow rate of 300 cm³/min. For comparison, the low-*k* films were also deposited without carrier gas from the mixture of 3MS and O_2 (referred to as STD). The optimal 3MS/O_2 gas ratio was 6. The deposition pressure and RF power were maintained at 533 Pa and 600 W, respectively, throughout the deposition process. The deposition temperature was varying from 200 to 400 °C.

Film thickness and refractive index (RI, at 633 nm wavelength) were measured by reflectometer and/or ellipsometer using the Nano-Spec®9100. Forty-nine point measurements were conducted on each wafer and the uniformity is defined herein as

$$Uniformity = \frac{Std.}{M} \times 100\% \qquad (1)$$

where Std. is the standard deviation and M is the mean value from the 49-point measurements. Chemical bonding of the

film was investigated using Fourier transform infrared spectroscopy (FT-IR) [Bio-Rad Win-IR PRO] and X-ray photoemission spectroscopy (XPS) using the 30-nm-thick film deposited on an 8-in. silicon wafer. XPS measurements were performed in a VG Microlab 310F system utilizing an MgKα X-ray source. The MTS Nano Indentor was used to measure the nano-hardness and Young's modulus of these films. The sample thickness for nano-hardness measurement was approximately 1 μm. The depth penetration was about 100 nm at ~0.3 mN down force, and each hardness entry is the average over five measurements. Dielectric constant and leakage current were measured by mercury (Hg) probe current–voltage (*I–V*) and capacitance–voltage (*C–V*) methods (5100 CV system) at 1 MHz.

3. Results and discussion

For the CVD reaction mechanism, the reaction sequence can be separated into several sequential steps. For the 3MS/O_2 low-*k* film deposition process used in this study, exhibited in Fig. 1, 3MS and O_2 were used in the gas phase under the plasma environment to form the intermediate compounds, which could further react with O_2 to form by-products. The forming intermediates then diffuse through
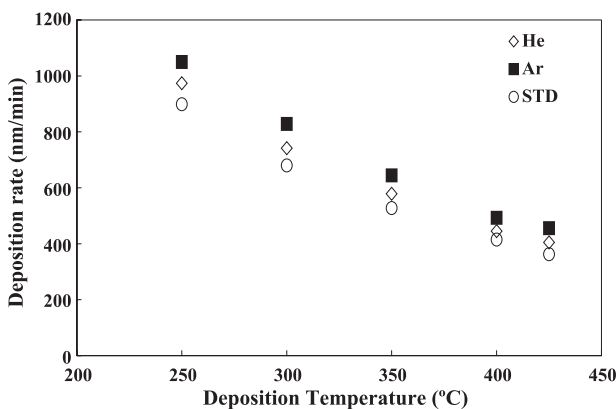
Fig. 2. The effects of the deposition temperature on the deposition rate of the low-*k* film processes.
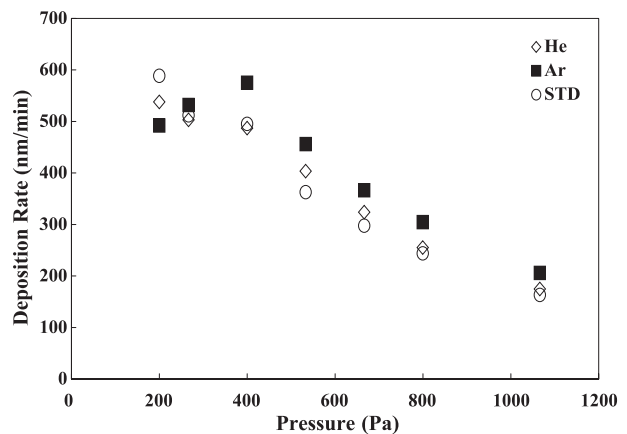
Fig. 3. The effects of the deposition pressure on the deposition rate of the low-*k* film processes.

Table 1
Physical properties of the He and Ar carrier gases

Carrier gas	Ionization energy (eV)			Molecular weight (a.m.u.)	Lennard-Jones collision diameter (Å)	Mass diffusivity (cm²/s)	Thermal conductivity (cal/cm s K)
	First	Second	Third				
He	24.59	54.42		4	2.551	13.43	4.68×10^{-4}
Ar	15.76	27.63	40.74	40	3.542	3.15	9.03×10^{-4}

Ionization energy denotes the ionization energy of the nth electron.

the gas media, which is mostly composed of an O radical and a carrier gas (if Ar or He was introduced), and are adsorbed onto the substrate, undergoing surface migration and reaction to form the low-k film. Other by-products desorb from the substrate surface and diffuse into the gas phase.

The reaction mechanism is mainly divided into three major process steps, the gas phase reaction, the gas phase diffusion, and the surface reaction. Each of the process steps in the reaction process has its own characteristics and depends on the process conditions used: (i) gas phase reaction relies on a function of the chamber pressure, reactant concentration (controlled by gas flows), and temperature inside the gas phase, which depends on the thermoconductivity of the gas phase molecules; (ii) gas phase diffusion is affected by the distance traveled by the intermediates, which scales with susceptor spacing. The mean free path (or diffusion coefficient) is a function of gas molecular size and chamber pressure; (iii) surface processes including adsorption, migration, surface reaction, and desorption are functions of the surface temperature and less affected by the total pressure inside the chamber. All three major steps are the series reaction steps. Based on the kinetic theory, the film deposition rate is the net effect of all the above steps, including gas phase reaction, diffusion, and surface reactions, and it is limited by the step with the slowest forming rate. Therefore, investigation of the deposition rate helps identify the restricting step and optimize the conditions for this process.

The temperature dependence of deposition rate of the low-k films with various types of carrier gases is shown in Fig. 2. The deposition pressure and RF power were set at

533 Pa and 600 W, respectively. Regardless of the type of the carrier gas, the low-k film deposited using 3MS and O_2 gases displays a very strong surface temperature effect and follows a similar kinetic reaction mechanism. The decreasing deposition rate suggests the importance of the surface adsorption and desorption. Moreover, the activation energy of the reaction can be determined by the Arrhenius equation shown as follows.

$$R = A\exp(-E_a/KT) \tag{2}$$

where R is the deposition rate, A is the Arrhenius constant, E_a is the reaction activation energy, K is the Boltzmann constant, and T is the absolute temperature. From Eq. (2), the activation energy for the low-k films with different carrier gases is comparable. The values are 0.642 and 0.666 eV for Ar and He carrier gases, respectively. On the other hand, the deposition rate of the low-k film using dilute Ar gas is clarified to be larger than that of He or without any carrier gases. The causes are (i) the carrier gas can rapidly ionize the reactants, 3MS and O_2, to form radicals and increase the concentration of the reactants. (ii) The ionization voltage of Ar gas is lower than that of He carrier gas, indicating that He gas is scarcely ionized. Therefore, compared to Ar carrier gas, the plasma strength in the process chamber using He is rather weaker. In addition, the uniformity of low-k film thickness [obtained from Eq. (1)] can be reduced from 2.5% to 1.5% as a result of uniform plasma distribution for Ar carrier gas. This nonuniformity of thickness or RI causes the large variations in device performance depending on the location of the wafer. The low-k films deposited using 3MS, O_2, and Ar carrier gas have a more uniform thickness and dielectric constant from the center to the edge location of the wafer, which may be caused by a uniform plasma density across the wafer as Ar gas is incorporated into the reaction.

Further investigation of the effect of carrier gas on the low-k film was performed to study the deposition mechanism. Fig. 3 shows that the deposition rate varies
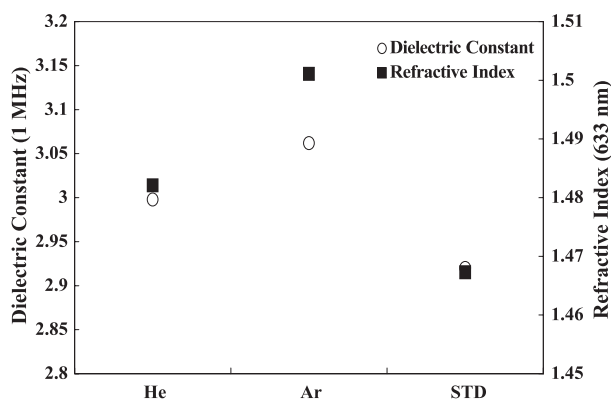

Fig. 4. The effects of carrier gas on the dielectric constant and refractive index of the low-k films.

Table 2
Percentage of element of the deposited SiCOH films under different carrier gases by XPS quantification (%)

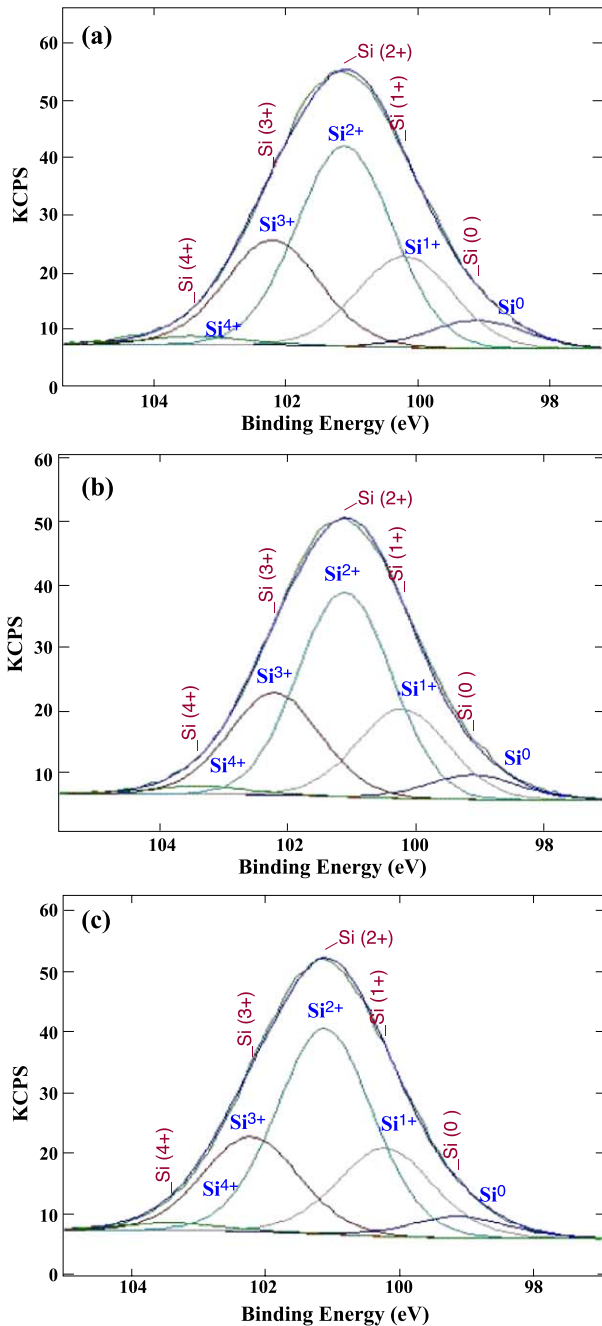| Carrier gas	Take-off 0°			Take-off 60°		
	O	C	Si	O	C	Si
He	34.7	30.9	34.4	34.3	33.1	32.7
Ar	33.1	31.8	35.1	33.4	34	32.6
STD	33.6	31.6	34.8	33.1	33.2	33.8

Fig. 5. Binding energy of Si^{2p} spectrum for the low-k films using (a) STD (without carrier gas); (b) He carrier gas; (c) Ar carrier gas.

Ar carrier gas, an optimized deposition rate is achieved as the chamber pressure changes. This can be interpreted as a change in the controlling step from reaction-limited to diffusion-limited step. In a low-pressure region (<400 Pa), the reaction rate is relatively slow, due to insufficient gas phase intermolecular collision. However, a faster diffusion rate is due to the long mean free path of the intermediates. Therefore, gas phase reaction controls the total deposition rate. In contrast, with either He carrier gas or without a carrier gas, a strong pressure effect is exhibited. The deposition rate is increased with decreasing the pressure. The reason for the difference between Ar and He carrier gas is the mean free path of the intermediates, resulting from the differences of the molecular size and collision diameter. Table 1 shows the physical properties of Ar and He gases.

Fig. 4 compares the relationship between the dielectric constant (k value) and the refractive index of the low-k films using Ar or He carrier gases. As compared to the low-k film without a carrier gas, the k values of low-k films using Ar or He carrier gas are found to be slightly larger. Furthermore, the k value using Ar carrier gas is larger than that of He carrier gas at the same deposition pressure and temperature. From the FTIR absorption peak height ratio between the Si–CH$_3$ and Si–O bonds, a higher value is calculated using Ar carrier gas. The higher Si–CH$_3$ content in the low-k film is known to lead to the lower k value in most cases. However, this result conflicts with the k value shown in Fig. 4. It is worth noticing that the reduction of dielectric constant of the low-k film is attributed to a less polarization of Si–CH$_3$ bonds and a microporous structure. It is believed that the refractive index of a dielectric film reflects its density. A lower film density means it contains a more microporous structure. As a result, when the carrier gas (Ar or He) is introduced into the process chamber, the k value reduction of the deposited film is contributed from Si–CH$_3$ bonds and microporous voids. As shown in Fig. 4, the low-k film using Ar carrier gas has a higher refractive index, which means this low-k film has a less microporous structure. In spite of the higher Si–CH$_3$ bonds, the low-k film with Ar carrier gas has a higher k value resulted from the microporous structure dominant in the reduction of the k value. The velocity of He is faster than that of Ar. As a result, He gas easily collides with 3MS that contains Si–CH$_3$ bonds, reducing the bonds in the precursor. On the other hand, Ar gas has a bombardment effect, to densify

with the deposition pressure. A drastic difference in the pressure dependence of deposition rate of the low-k films with different carrier gases can be observed in Fig. 3. For

Table 3
Related binding energy and percentage for Si^{2p} peak

Si(2p)	Si^{4+}–O$_4$	Si^{4+}–O$_3$	Si^{4+}–O$_2$	Si^{4+}–O$_1$	Si^{4+}–O$_0$
Binding energy (eV)	103.4	102.2	101.1	100.2	99.1
He	2%	23%	49%	21%	5%
Ar	2%	24%	47%	21%	6%
STD	2%	24%	48%	21%	6%

the low-k film. Therefore, a lower k value indicates that the deposited film using He carrier gas has more voids than that using Ar carrier gas.

To further investigate the role of the carrier gas on the chemical structure of low-k films, XPS was used to address the differences in the chemical structure. Table 2 lists the percentage of elements from XPS quantification. Films deposited by the carrier gases were determined to have a similar atomic ratio although there is still a slight increase in carbon atoms for the Ar carrier gas. This result matches with the result acquired from FTIR analyses. Furthermore, we deconvoluted the Si (2p) spectra into the five main moieties using a curve-fitting method, as indicated in Fig. 5. These five chemical distinct Si atoms arise from SiO_4 (103.4 eV), SiO_3 (102.2 eV), SiO_2 (101.1 eV), SiO_1 (10.2 eV) and SiO_0 (99.1 eV), respectively. Table 3 compares the Si (2p) spectra bonding energy of films deposited using various carrier gases. As shown in Table 3, all films exhibit a similar structure, resembling the FTIR spectrum. This indicates that the dominant Si binding energy is about 101.1 eV. As a consequence, it is implied that the main bonding of the films is –O–Si–O–Si–.

Fig. 6 shows the leakage current density of the low-k films deposited using different carrier gases. The deposition pressure and RF power were 533 Pa and 600 W, respectively. It is found that the leakage current density of the low-k film deposited using Ar carrier gas is slightly lower than that of He carrier gas or without a carrier gas. The lower leakage current density of the low-k film using Ar carrier gas is a result of less porosity in the film. Additionally, the leakage current densities of the low-k films are approximately 10^{-9} A/cm^2 in an electric field of 2 MV/ cm in our study, which are similar to other studies [9–11].

Fig. 7 compares the dry etching rate of the low-k films deposited using various carrier gases. The dry etching
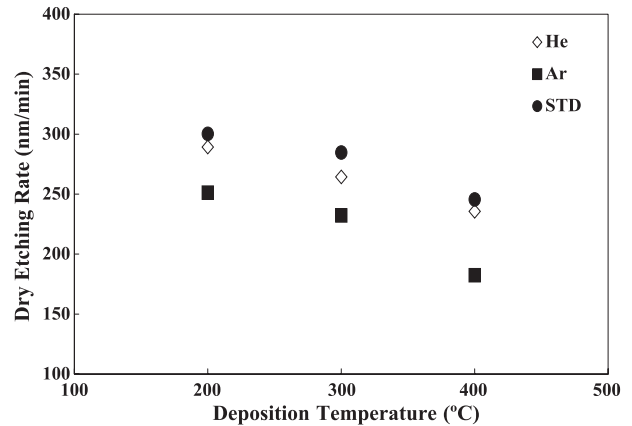

Fig. 7. The dry etching rate of the low-k films as a function of deposition temperature with different carrier gases.

process was performed under reactive ion etching processes using $CF_4/CHF_3/N_2/Ar$ as the reactant gases. The influence of the carrier gas on the dry etching rate is obvious as shown in Fig. 7. The lowest and highest etching rate is obtained with Ar carrier gas and STD condition (without carrier gas), respectively, implying that the deposited low-k film using Ar carrier gas has a higher film density and a lower porosity. It suggests that the low-k film deposited in Ar plasma ambient is suitable for the intermetallic-dielectric (IMD) layer because the metal-trench depth has less variation and can be well-controlled in a dual-damascene structure without a trench stopping scheme process.

Low hardness of the low-k film causes a peeling issue during the copper chemical mechanical polishing (Cu-CMP) processes. Therefore, the hardness of the low-k film should be taken into account as the low-k film is implemented into multilevel metallization. Mechanical hardness and Young's modulus of the low-k films deposited with different carrier gases are plotted as a function of the deposition temperature
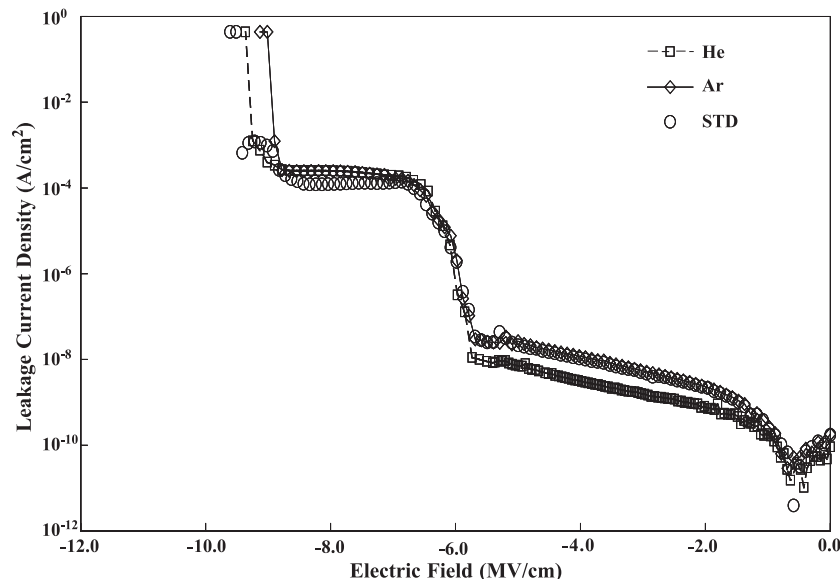

Fig. 6. The leakage current density of the low-k films deposited using different carrier gases.
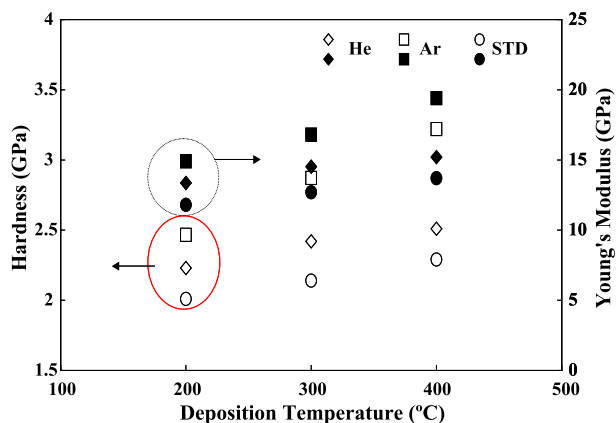
Fig. 8. The hardness and Young's modulus of the low-*k* films with different carrier gases.

as shown in Fig. 8. It is noted that the hardness of the low-*k* film deposited with Ar carrier gas is higher than that of the other two deposition conditions for all temperature ranges. This result proves that the low-*k* film with Ar carrier gas is more suitable for the implementation as an IMD low-*k* film due to its high mechanical strength against the Cu-CMP processes. Fig. 8 clearly indicates a trend on the improvement in hardness as well as Young's modulus when the deposition temperature is increased. However, the dielectric constant of the deposited film is increased with raising the deposition temperature. The hardness and the dielectric constant of the low-*k* film show a trade-off depending on the deposition temperature. Consequently, it is essential to reach a compromise between the dielectric constant and the mechanical strength when the deposition temperature is determined.

4. Conclusions

PE-CVD low-*k* films utilizing 3MS and O_2 as source reactants and Ar or He as the carrier gas were characterized in this study. The deposition rate of the low-*k* film is increased as the carrier gas was introduced. However, a slight degradation on the dielectric constant of the deposited low-*k* films was occurred. Also, low-*k* films with Ar carrier gas exhibited the strong improvement in deposition rate, nonuniformity, leakage current density, and hardness due to the decrease of micropores in the deposited films.

References

[1] L.M. Han, J.S. Pan, S.M. Chen, N. Balasubramanian, J. Shi, L.S. Wong, P.D. Foo, J. Electrochem. Soc. 148 (2001) F148.
[2] Q. Wu, K.K. Gleason, J. Vac. Sci. Technol., A, Vac. Surf. Films 21 (2003) 388.
[3] R. Suzuki, T. Ohdaira, Y. Shioya, T. Ishimaru, Jpn. J. Appl. Phys. 40 (2001) 414.
[4] V. Ligatchev, T.K.S. Wong, B. Liu, T. Rusli, J. Appl. Phys. 92 (2002) 4605.
[5] A. Grill, V. Patel, J. Appl. Phys. 85 (1999) 3314.
[6] T.C. Chang, Y.S. Mor, P.T. Liu, T.M. Tsai, C.W. Chen, Y.J. Mei, S.M. Sze, J. Electrochem. Soc. 149 (2003) F81.
[7] K.M. Chang, S.W. Wang, C.H. Wang, C.H. Li, T.H. Yeh, Y. Yang, Appl. Phys. Lett. 70 (1997) 2556.
[8] P.T. Liu, T.C. Chang, H. Su, Y.S. Mor, Y.L. Yang, H. Chung, J. Hou, S.M. Sze, J. Electrochem. Soc. 148 (2001) F30.
[9] T.C. Chang, P.T. Liu, H. Su, Y.S. Mor, Y.L. Yang, H. Chung, J. Hou, S.M. Sze, J. Vac. Sci. Technol., B 20 (2002) 1561.
[10] Y. Shioya, Y. Kotake, T. Ishimaru, T. Masubuchi, H. Ikakura, K. Maeda, J. Electrochem. Soc. 150 (2003) F1.
[11] N. Yamada, T. Takahashi, J. Electrochem. Soc. 147 (2000) 1477.